In the response evaluation criteria in solid tumors (RECIST), CT and magnetic resonance imaging (MRI) are considered the best currently available and the most useful tools for assessing the therapeutic effect on the target lesions, and the maximum diameter for the target lesions used as the reference to the objective tumor response [10]. However, the limited value of the RECIST criteria has been pointed out. PET with [^{18}F]-fluoro-2-deoxy-glucose (18F-FDG) has been used in the evaluation of patients with solid tumors, because the metabolic reduction precedes morphological changes [11]. Most studies on therapeutic response reveal that 18F-FDG-PET is superior in the assessment of therapeutic monitoring compared with conventional imaging [12–15]. PET has the potential to therapy monitoring in patients with cervical carcinoma. However, the exact role of ^{11}C-choline PET scan in the assessment of tumor response for cervical carcinomas has not been elucidated fully.

Positron emission tomography/computed tomography can improve tumor localization and staging accuracy because the anatomic and molecular information can be precisely co-registered [16]. The aim of the current study was to clarify the exact role of ^{11}C-choline PET/CT in the management of uterine carcinoma.

Materials and methods

Patients

We retrospectively reviewed the results of ^{11}C-choline PET/CT from January 2006 to December 2006 in patients with uterine carcinoma who either underwent radical hysterectomy and pelvic lymphadenectomy or were started on chemotherapy within a week. ^{11}C-choline PET/CT had been performed only for patients who had provided written informed consent to participate in the study and to a review of their records and images. A total of 22 patients with uterine carcinoma (cervical carcinoma, $n = 11$; corpus carcinoma, $n = 11$), which included preoperative studies for initial staging in all 22 patients, were enrolled into this study. In five patients with cervical carcinoma, both initial and follow-up examinations after chemotherapy in five patients were performed. The mean age was 51 years (range 31–73 years). The clinical records of all 22 patients were available for review. This study was conducted in accordance with the amended Helsinki declaration, and the protocol was approved by the Institutional Review Board.

PET/CT

Studies were performed with the LSO-based whole-body PET/CT scanner (Aquiduo;Toshiba). The CT component of the scanner was the same as that of Aquillion 16, which has 16-rows detector. The PET component of the scanner has a transaxial field of view of 68.3 cm and an axial field of view of 16.2 cm without septa and rotating rod source. The scanner was used in 3D mode with image resolution of 4.0 mm in full width at half maximum (FWHM). Prior to the ^{11}C-choline PET/CT study, the patients fasted for at least 6 h. CT was performed from the head to the mid-thigh according to a standardized protocol with the following settings: axial 2.0-mm collimation × 16 modes; 120 kVp; Auto-Exposure Control (SD10); and a 0.5-s tube rotation, a table speed of 11.0 mm/s. Patients maintained normal shallow respiration during the acquisition of CT scans. No iodinated contrast material was administered. ^{11}C-choline was synthesized with a commercial module described by Hara and co-workers [17]. Acquisition of emission scans from the head to the mid-thigh was started 5 min after intravenous administration of a mean ^{11}C-choline dose of 464 MBq (range, 409-560 MBq). Second emission scans of the pelvis were subsequently obtained starting 17 min of uptake time. The acquisition time for PET was 2 min per table position. Images were reconstructed with attenuation-corrected ordered-subset expectation maximization with 4 iterations and 14 subsets using emission scans and CT data.

Magnetic resonance imaging

MRI was performed within 2 weeks of ^{11}C-choline PET/CT, both before and after treatment. MRI was performed using a 1.5 T system (Signa Horizon LX, GE Medical Systems, Milwaukee). Pulse sequences comprised T1-weighted spin echo (SE) images (TR (repetition time)/TE (echo time): 500–600 ms/7–10 ms), T2-weighted fast spin echo (FSE) images (TR/TE: 3,750–4,400 ms/98–105 ms), as well as post-contrast T1-weighted SE images (TR/TE: 580–645 ms/6–10 ms) with fat suppression after injection of contrast material. All images were acquired in the transverse plane with a slice thickness of 5.0 mm, and a 1.0 mm intersection gap. The contrast material used was gadopentetate dimeglumine (Magnevist, Bayer Schering Pharma, Osaka, Japan) at a dose of 0.1 mmol/kg body weight. Pulse sequence parameters and slice orientation varied with the examined anatomic site. The images were reviewed and a consensus was reached by two board-certified radiologists who were unaware of any clinical or radiological information using multimodality computer platform.

Image interpretation

The images were reviewed by a board-certified radiologist and a nuclear medicine specialist who were unaware of any clinical information and a consensus was reached. PET,

CT, MRI, and co-registered PET/CT images were analyzed with dedicated software (e-soft; Siemens). PET, CT, and MRI were interpreted separately and co-registered PET/CT was read 6 months after the initial review. ^{11}C-choline uptake was considered abnormal when substantially greater than that of the surrounding normal tissue. A region of interest (ROI) of 1 × 1–3 × 3 pixels was manually outlined within regions of increased ^{11}C-choline uptake and measured on each slice. For quantitative interpretations, the standardized uptake value (SUV) was determined according to the standard formula, with activity in the ROI recorded as Bq per ml/injected dose in Bq per weight (kg), but time decay correction for whole-body image acquisition was not performed. The maximum SUV (SUV max) was recorded using the maximum pixel activity within the ROI. We obtained 40% of maximum counts as the activity threshold. Both SUV max at a mean uptake time of 5 and 17 min were recorded as SUV_1 and SUV_2, respectively. The change in SUV was also calculated according to the formula: δ SUV (%) = $(SUV_1 - SUV_2)/SUV_1 \times 100$. Uni-dimensional and volumetric measurements were conducted on MRI by the single radiologist. On the uni-dimensional measurement, tumor size was defined as the maximum diameter. On the volumetric measurement, tumor volume was calculated by a slice-by-slice evaluation. The area of the tumor was manually measured slice-by-slice on the transaxial post-contrast T1-weighted SE images with fat suppression, using manual segmentation with the multimodality computer platform. The measured area (cm^2) per slice was multiplied by the factor 0.6 cm. The factor of 0.6 cm is based on the slice thickness of 5 mm and a distance factor of 1 mm. The volume of all measured slices containing tumor was summed up for total tumor volume.

Staging in cervical carcinoma

Tumor size by ^{11}C-choline PET/CT was determined based on the CT portion of the PET/CT. In tumors with unclear contour, tumor size was determined as the diameter of the cervix. T1 was considered when localized tumor with ^{11}C-choline uptake was depicted in the cervix. T2 was considered when tumor invaded the parametrium with ^{11}C-choline uptake for cervical carcinoma. T3 was considered when tumor with ^{11}C-choline uptake involved the serosa, adnexa, vagina, or peritoneal dissemination. Lymph nodes with abnormal uptake were recorded as positive for metastasis even when their short-axis diameter was less than 10 mm. N stage in six patients was confirmed by pathologic examination of specimens obtained by sampling of regional nodes. Nodal status of extraregional lymph nodes was confirmed in five patients by obvious regression in size of the lesions on follow-up MR examinations after treatment. M stage was determined when paraaortic lymph node was involved or distant metastasis was found on contrast-enhanced CT during follow-up.

Staging in corpus carcinoma

Tumor size was also determined based on the CT portion of the PET/CT. In tumors with unclear contour, tumor size was determined as the diameter of the corpus. T1 was considered when localized tumor with ^{11}C-choline uptake was depicted in the corpus. T2 was considered when tumor involved the cervix with ^{11}C-choline uptake. T3 was considered when tumor with ^{11}C-choline uptake involved the serosa, adnexa, vagina, or peritoneal dissemination. Lymph nodes were classified similarly to those of cervical carcinoma. N stage was confirmed by pathologic examination of specimens obtained by sampling of regional nodes in all patients. M stage was determined when distant metastasis was found on contrast-enhanced CT during follow-up.

Treatment

In five patients with cervical carcinoma, treatment consisted of cisplatin infusion and subsequent radiotherapy. All but one of the patients, except one, were received chemotherapy consisting of cisplatin. One patient who had renal dysfunction did not receive chemotherapy. Radiotherapy comprised external beam radiotherapy (EBRT) 50 Gy and intra-cavitary radiotherapy (ICRT) 18–24 Gy. EBRT of the whole pelvis was performed and a total dose of 50 Gy was delivered at the rate of 2 Gy per fraction in 5 weeks. ICRT was performed and a total dose of 18–24 Gy was delivered at the rate of 8 Gy per fraction once a week. Four patients underwent chemotherapy with cisplatin (range 56–63 mg; mean 60.3 mg) once a week during EBRT. ^{11}C-choline PET/CT scans were performed before the start of treatment and after treatment.

Assessment of therapeutic response

The tumor size and volume from MRI after treatment were compared with those from the baseline study. The percentage of size reduction rate (%Size-RR) was calculated by the following formula; [Size (baseline) – Size (after treatment)]/Size (baseline) × 100 (%). The percentage of volume reduction rate (%Volume-RR) was calculated by the following formula; [Volume (baseline) – Volume (after treatment)]/Volume (baseline) × 100 (%).

Evaluation of metabolic response was accomplished by comparing the relative change in SUV, the percentage of SUV reduction rate (%SUV-RR). The SUV_1 and the SUV_2 from ^{11}C-choline PET/CT after treatment were compared with the baseline study. The percentage SUV_1 reduction

rate (%SUV_1-RR) was defined as the following formula; [SUV_1 (baseline) − SUV_1 (after treatment)]/SUV_1 (baseline) × 100 (%). The percentage SUV_2 reduction rate (%SUV_2-RR) was defined as the following formula; [SUV_2 (baseline) − SUV_2 (after treatment)]/SUV_2 (baseline) × 100 (%).

Statistical analysis

Each tumor was staged according to the TNM classification of the International Union Against Cancer (UICC) and the International Federation of Gynecology and Obstetrics (FIGO) Committee on Gynecologic Oncology [18, 19]. The mean follow-up period was 240 days (range 53–425 days). All variables were assessed on a patient-by-patient basis. Student's *t* test was used for paired comparisons of SUV. The McNemar test with Bonferroni's correction was used for paired comparisons between the results obtained by staging of ^{11}C-choline PET/CT. Therapeutic response was compared with imaging parameters using the Pearson correlation test. Correlation at a *P* value of less than 0.05 was considered to indicate a statistically significant difference. All data analysis was performed using software package SPSS 16.0J (SPSS, Chicago, IL, USA).

Results

Staging in cervical carcinoma

There were 11 cervical carcinomas (Table 1). Their histologic diagnoses were squamous cell carcinoma ($n = 8$), small cell carcinoma ($n = 2$), and adenosquamous carcinoma ($n = 1$). The tumor size of cervical carcinomas was 35 ± 14 mm. T stage was T1 in 2 patients (18%), T2 in 4 patients (36%), T3 in 3 patients (27%), and T4 in 1 patient (6%). The patient with T4 disease had rectal invasion microscopically. T stage was correctly classified by MRI alone in 6 patients (100%), by PET/CT alone in 3 patients (50%), and by PET/CT plus MRI in 6 patients (100%). Six (55%) of the 11 patients had N1 disease (Table 2). The accuracy of N staging was 73% by MRI alone, 91% by PET/CT alone, and 91% by PET/CT plus MRI. One patient had M1 disease with involvement of a paraaortic lymph node. The accuracy of M staging was 100% by PET/CT plus MRI as well as by PET/CT alone.

Staging in corpus carcinoma

The histologic diagnoses of 11 corpus carcinomas (Fig. 1) were endometrioid adenocarcinoma ($n = 9$), carcinosarcoma ($n = 1$), and serous adenocarcinoma ($n = 1$). The histologic grades of the corpus carcinomas were Grade 1 ($n = 6$), Grade 2 ($n = 3$), and Grade 3 ($n = 2$). No significant differences in SUV_1 ($p = 0.236$) or SUV_2 ($P = 0.348$) of the primary lesion were found between cervical carcinoma and corpus carcinoma (Fig. 1). The δSUV in each type of tumor was similar at both primary sites ($P = 0.347$). The tumor size of the corpus carcinomas was 36 ± 21 mm. T stage was T1 in 5 patients (45%), T2 in 1 patient (6%), and T3 in 5 patients (45%). T stage was correctly classified by MRI alone in 9 patients (82%), by PET/CT alone in 5 patients (45%), and by PET/CT plus MRI in 10 patients (91%). One patient with corpus carcinoma who had developed a vaginal metastasis was understaged by MRI alone. After adding interpretation of PET/CT which showed discrete uptakes in the corpus and

Table 1 Demographic data of patients with cervical and corpus carcinomas

Parameter	Cervical carcinoma	Corpus carcinoma	Total
No. of patients	11	11	22
Age			
Mean ± SD	49 ± 12	53 ± 12	51 ± 12
Range	33–68	31–73	31–73
SUV_1			
Mean ± SD	4.83 ± 1.87	5.92 ± 2.30	5.37 ± 2.12
Range	2.06–9.42	2.71–9.31	2.06–9.42
SUV_2			
Mean ± SD	4.98 ± 1.97	5.82 ± 2.10	5.40 ± 2.04
Range	2.30–10.01	3.00–9.31	2.30–10.01
δSUV (%)			
Mean ± SD	−4.05 ± 14.01	0.40 ± 6.28	−1.82 ± 10.84
Range	−39.67–14.25	−10.70–14.00	−39.67–14.25
Final stage	IB ($n = 2$)	IA ($n = 1$)	
	IIB ($n = 4$)	IB ($n = 4$)	
	IIIB ($n = 3$)	IIA ($n = 1$)	
	IVB ($n = 1$)	IIIA ($n = 2$)	
		IIIB ($n = 1$)	
		IIIC ($n = 2$)	

SD standard deviation, *SUV_1* SUV at a mean uptake time of 5 min, *SUV_2* SUV at a mean uptake time of 18 min

Table 2 Location of metastatic lymph nodes in all patients

Lymph node	No. of patients
Obturator	8 (36.3)
Common iliac	3 (13.6)
Paraaortic	2 (9.0)
External iliac	2 (9.0)
Internal iliac	2 (9.0)
Suprainguinal	1 (4.5)

The numbers in parentheses are percentages

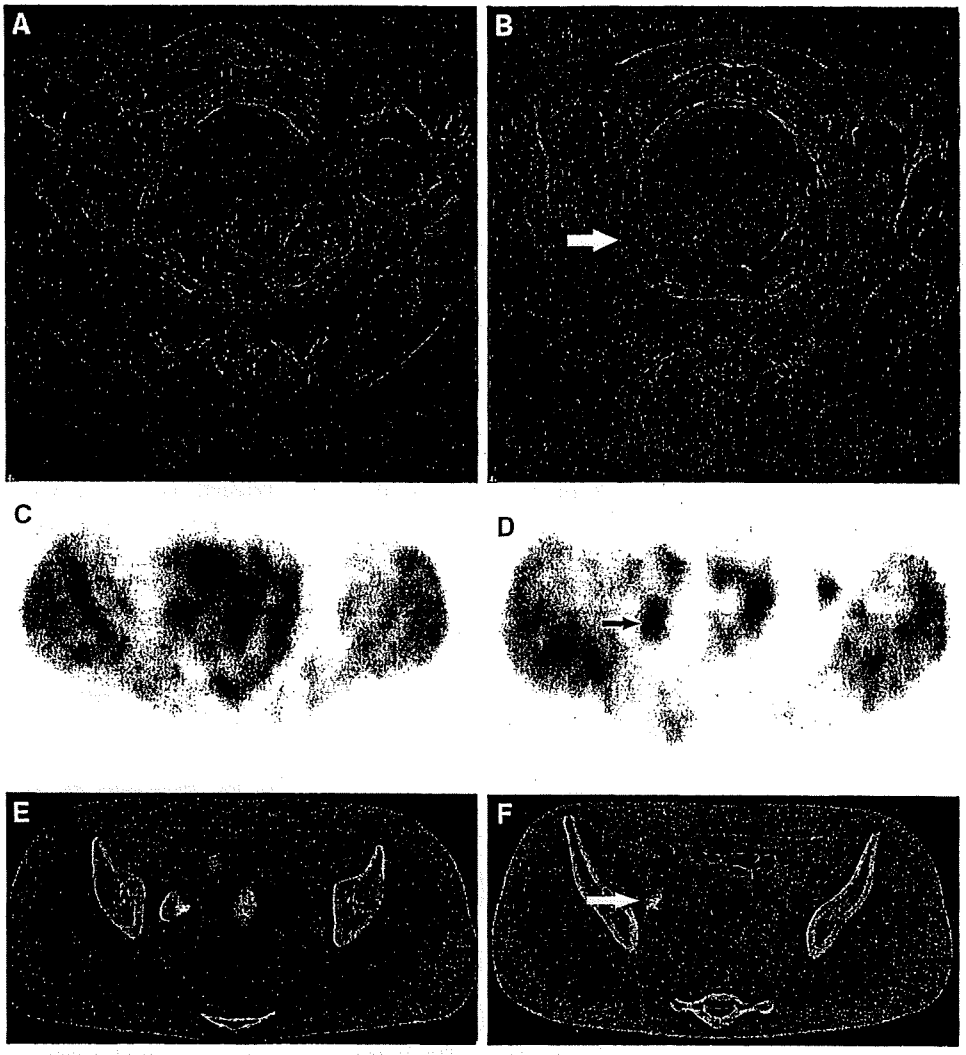

Fig. 1 A 52-year-old woman with corpus carcinoma. **a, b** Transverse T2-weighted MR image (TR/TE_{eff}: 4,000 ms/100 ms) shows a primary tumor of the isthmus and enlargement of the right obturator lymph node (*arrow*). **c, d** Transverse ^{11}C-choline PET image reveals a hypermetabolic focus in the primary tumor and right obturator region (*arrow*). **e, f** Transverse ^{11}C-choline PET/CT image reveals a hypermetabolic focus in the primary tumor and right obturator lymph node (*arrow*). PET/CT findings were verified by histopathologic analysis

vagina, this patient was correctly diagnosed as having a vaginal metastasis. A patient with corpus carcinoma and peritoneal dissemination was understaged by MRI alone, whereas staging by PET/CT alone or PET/CT plus MRI was correct. Three (27%) of the 11 patients had N1 disease. The accuracy of N staging was 64% by MRI alone, 82% by PET/CT alone, and 100% by PET/CT plus MRI. All patients had M0 disease. The accuracy of M staging was 91% by PET/CT plus MRI and 82% by PET/CT alone. PET/CT alone overstaged two patients with corpus carcinoma as having distant metastasis, and their definitive diagnosis was vaginal metastasis and normal paraaortic lymph node, respectively. One patient with corpus carcinoma was overstaged by PET/CT plus MRI as having M1 disease.

Staging performance in uterine carcinomas

T stage (Table 3) was correctly classified by MRI alone in 15 patients (88%), by PET/CT alone in 8 patients (47%), and by PET/CT plus MRI in 16 patients (94%). MRI alone or PET/CT plus MRI was superior to PET/CT alone in determining T stage ($P = 0.039$ or $P = 0.008$, respectively). PET/CT alone understaged four patients and overstaged five patients: The accuracy of N staging (Table 3) was 68% by MRI alone, 86% by PET/CT alone, and 96% by PET/CT plus MRI. PET/CT plus MRI was superior to MRI alone in assigning N stage ($P = 0.031$). MRI alone understaged four patients with subcentimetric lymph node and overstaged three patients with reactive lymph nodes. However, PET/CT alone understaged two patients with lymph node fewer than 10 mm in diameter and overstaged one patient with reactive lymph node. One patient with a lymph node was understaged by PET/CT plus MRI. The accuracy of M staging (Table 3) was 96% by PET/CT plus MRI and 91% by PET/CT alone. The overall stage (Table 3) was correctly diagnosed by PET/CT in 47%, and by PET/CT plus MRI in 88% ($P = 0.039$). PET/CT alone led to assignment of an incorrect TNM stage in nine patients due to misdiagnosis of T stage. Two patients were incorrectly diagnosed by PET/CT plus MRI.

Consequently, the misdiagnoses were in a patient with corpus carcinoma who had vaginal metastasis and a patient with a lymph node that measured fewer than 10 mm in diameter.

Table 3 Comparison of the diagnostic accuracy of staging by MRI, PET/CT, and combining PET/CT and MRI (PET/CT+MRI)

Diagnosis	MRI	PET/CT	PET/CT+MRI
T stage ($n = 17$)			
Correct	15 (88.2)*	8 (47.1)*†	16 (94.1)†
Overstaged	0	5 (29.4)	0
Understaged	2 (11.8)	4 (23.5)	1 (5.9)
N stage ($n = 22$)			
Correct	15 (68.2)†	19 (86.4)	21 (95.5)†
Overstaged	3 (13.6)	1 (4.5)	0
Understaged	4 (18.2)	2 (9.1)	1 (4.5)
M stage ($n = 22$)			
Correct	NA	20 (90.9)	21 (95.5)
Overstaged	NA	2 (9.0)	1 (4.5)
Understaged	NA	0	0
Overall stage ($n = 17$)			
Correct	NA	8 (47.1)†	15 (88.2)†
Overstaged	NA	5 (29.4)	1 (5.9)
Understaged	NA	4 (23.5)	1 (5.9)

The numbers in parentheses are percentages. The diagnostic accuracy of two modalities was compared by the McNemar test. Significant differences were found between two groups: * $P < 0.01$ and † $P < 0.05$

NA not applicable

Evaluation of therapeutic effect

Four (80%) of the five patients had IIb disease and one patient (20%) had IVa disease. One patient with IVa disease had bladder invasion and suffered from secondary bilateral hydronephrosis. Three patients (60%) had pelvic lymph node enlargement. Two of them were detected in bilateral obuturator enlarged lymph nodes, and the other in right obuturator enlarged lymph node. Distant metastases were not detected in any patients.

Baseline MRI showed that tumor size was 36.5 ± 8.7 mm. After treatment, the mean size was reduced to 21.8 ± 8.2 mm. Baseline MRI showed a tumor volume of 20.2 ± 12.6 cm^3. After treatment, the mean volume was reduced to 12.2 ± 8.4 cm^3 (Fig. 2). The %Size-RR was 40.7 ± 12.8% and the %Volume-RR was 56.5 ± 10.3% (Table 4).

All five patients had abnormal ^{11}C-choline uptake of the primary lesion on initial PET/CT. SUV_1 and SUV_2 after chemoradiotherapy decreased compared with that before chemoradiotherapy. Baseline PET/CT showed a mean SUV_1 of 5.3 ± 2.4, and a mean SUV_2 of 5.2 ± 2.7. After treatment, the SUV_1 decreased to 2.6 ± 1.2, and the SUV_2 decreased to 2.0 ± 1.0 (Fig. 2). The $\%SUV_1$-RR was 48.0 ± 20.0% and $\%SUV_2$-RR was 60.3 ± 14.4% (Table 5).

The correlation between $\%SUV_1$-RR and %Size-RR was not significant ($r = 0.698$, $P = 0.19$), while there was a significant correlation between $\%SUV_1$-RR and %Volume-RR ($r = 0.892$, $P = 0.042$). Indeed, there was

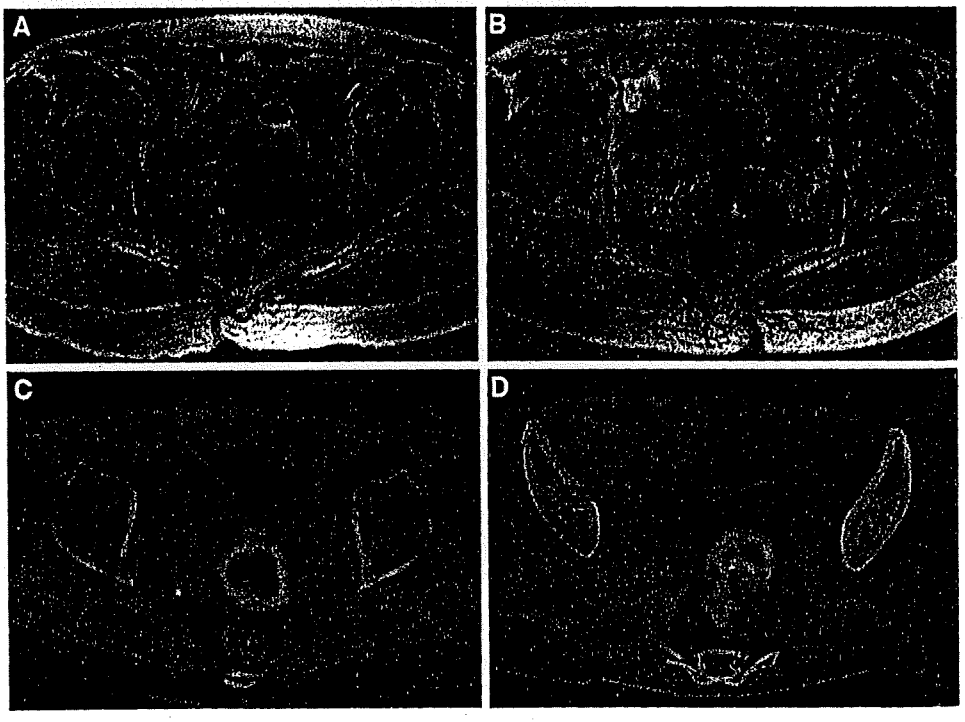

Fig. 2 A 60-year-old woman with cervical carcinoma: Transverse T2-weighted MR image on the baseline study (a) shows an isointense tumor of uterine cervix. The tumor size and volume are 32.6 mm and 12.59 cm^3, respectively. After treatment (b), the tumor is reduced in size. The tumor size and volume are 16.4 mm and 5.63 cm^3, respectively. Transverse ^{11}C-choline PET/CT image on the baseline study (c) shows an increased metabolic uptake in primary tumor. After treatment (d), metabolic uptake in the primary tumor decreases. The SUV_1 and SUV_2 decrease from 4.61 and 4.61 to 2:10 and 1.90, respectively

Table 4 Clinical characteristics in five patients with cervical carcinoma

Pt	Age	Chief complaint	Histology	Chemo		RT		Recurrence time (months)	Treatment after recurrence	Follow-up time (months)
				Dose (mg)	Cycle	EBRT	ICRT			
1	60	Vaginal bleeding	Squamous	56	1	50 Gy/25fr	18 Gy/3fr	3	Chemo	13
2	68	Vaginal bleeding	Squamous	0	0	50 Gy/25fr	18 Gy/3fr	8	None	14
3	55	Vaginal bleeding	Squamous	56	5	50 Gy/25fr	18 Gy/3fr	7	RT	16
4	35	Vaginal bleeding	Squamous	62.2	4	50 Gy/25fr	24 Gy/4fr	None	None	15
5	57	Vaginal bleeding	Squamous	63.4	4	50 Gy/25fr	18 Gy/3fr	None	None	13

Pt patient, *Chemo* chemotherapy, *RT* radiotherapy, *EBRT* extra body radiotherapy, *ICRT* intra cervical radiotherapy, *squamous* squamous cell carcinoma, *fr* fraction

Table 5 Assessment of MRI and 11C-choline PET results in five patients with cervical carcinoma

Pt	MRI							
	Diameter (mm)				Volume (cm^3)			
	Baseline	After	δ	RR (%)	Baseline	After	δ	RR (%)
1	32.6	16.4	16.2	49.7	12.59	5.63	6.96	55.3
2	40.7	28.4	12.3	30.2	31.64	14.78	16.86	53.3
3	45.5	32.7	12.8	28.1	21.37	8.57	12.81	59.9
4	23.3	14.5	8.8	37.8	2.99	1.71	1.28	42.9
5	40.6	17.1	23.5	57.9	32.27	9.27	23.01	71.3
Pt	^{11}C-choline PET							
	SUV_1				SUV_2			
	Baseline	After	δ	RR (%)	Baseline	After	δ	RR (%)
1	9.42	4.29	5.13	54.5	10.01	3.6	6.41	64
2	3.57	2.6	0.97	27.2	3.57	1.51	2.06	57.7
3	4.61	2.1	2.51	54.4	4.61	1.9	2.71	58.8
4	4.28	3.04	1.24	29	3.67	2.19	1.48	40.3
5	4.4	1.1	3.3	75	4.1	0.8	3.3	80.5

Pt patient, *Baseline* baseline study, *After* study after treatment, δ difference between baseline study and study after treatment, *RR* reduction rate

no significant correlation between %SUV_2-RR and %Size-RR ($r = 0.660$, $P = 0.226$), while there was a significant correlation between %SUV_2-RR and %Volume-RR ($r = 0.956$, $P = 0.011$). During a mean follow-up time of 14.2 ± 1.0 months, two patients developed disease recurrence. One patient had a local recurrence three months after the treatment, and received additional chemotherapy using cisplatin and paclitaxel. The other patient developed metastasis of a paraaortic lymph node seven months after the treatment, and received radiotherapy of the abdomen. No patients died before disease recurrence.

Discussion

The results of the present study show that ^{11}C-choline PET/CT contributes to accurate staging in patients with uterine carcinoma. Specifically, the combination of ^{11}C-choline PET/CT and MRI has potential implications for determining T and N stage at the preoperative evaluation. The results of the present study also indicate that ^{11}C-choline PET/CT may be feasible as a method of evaluating the therapeutic response after chemoradiotherapy in patients with cervical carcinoma.

Clinically, requirements for an acceptable method of preoperative staging of uterine carcinoma are that it allows determination of appropriate indications for surgery. Measured by this criterion, MRI has long been recognized as the most accurate modality, with high sensitivity [20, 21]. However, the limitation in MR evaluation for preoperative staging of uterine carcinoma is low specificity for N staging. In our study the interpretation of N staging by combining ^{11}C-choline PET/CT and MRI yielded an accuracy of 96%. The results of the present study suggest

that it will be feasible to diagnose preoperative nodal status in patients with uterine carcinoma. ^{11}C-choline PET/CT may complement MRI for diagnosing nodal status prior to operation in uterine carcinoma.

Physiological distribution of ^{11}C-choline uptake in vivo can affect signal-to-background ratio for imaging in malignant tumors. After intravenous administration of ^{11}C-choline, blood clearance is rapid and radioactive distribution in tissues reaches a steady state within five minutes. Normal uptake of ^{11}C-choline is observed in the liver, pancreas, kidney, duodenum, bone marrow, and secretion into phospholipid-rich pancreatic juice is also found in the non-fasting state. The physiological background level of ^{11}C-choline in the urinary tract is lower than that of 18-fluorodeoxyglucose (18F-FDG) because of incomplete tubular reabsorption of the intact tracer [22, 23] and enhanced excretion of labeled oxidative metabolites. Although we found one false-positive case for N staging by ^{11}C-choline PET/CT, this was attributable to a reactive lymph node on microscopic observation, not to ^{11}C-choline uptake in the urinary tract. Thus, accumulation of ^{11}C-choline in the pelvis is hardly affected by urinary uptake.

The limited spatial resolution and partial volume effect of PET/CT often result in failure to detect small lesions. In our study, two patients were understaged due to the presence of a metastatic lymph node fewer than 10 mm in diameter that was visualized by the CT portion of PET/CT or by MRI. Slight increases in tracer uptake and motion artifacts caused by respiration will give rise to false-negative results. On the other hand, the false-positive results were observed in one patient-by PET/CT and in three patients by MRI because of reactive lymph nodes. The advantage of the combining PET/CT and MRI was that it decreased the number of understaged and overstaged cases by correlating the morphologic and metabolic findings.

Evaluating the therapeutic response after chemoradiotherapy requires imaging modalities, such as CT or MRI that are generally standard. However, these anatomical imaging modalities have limitations, because it takes weeks or months to evaluate therapeutic response and it is difficult to distinguish residual tumor from fibrotic and necrotic tissue. Some investigators showed the efficacy of 18F-FDG-PET in monitoring therapeutic response in patients with cervical carcinoma [12–15]. Similar to the results of 18F-FDG-PET studies, all five patients had abnormal ^{11}C-choline uptake of cervical carcinoma on the baseline study, and had decreased ^{11}C-choline uptake compared with the baseline study after chemoradiotherapy in our study.

18F-FDG-PET-derived parameters including SUV and the percent change value may have the potential to predict the therapeutic response in patients with advanced gynecological cancer. Yoshida and colleagues reported that the decrease in SUV of 18F-FDG-PET was better correlated with histological response than was MRI in three patients with advanced cervical carcinoma after neoadjuvant chemotherapy. Similarly, the present study demonstrates that %SUV$_1$-RR and %SUV$_2$-RR calculated from ^{11}C-choline PET/CT correlated well with %volume-RR calculated from MRI.

Some limitations as to setup must be resolved before the results can be transposed to routine clinical settings. Our retrospective study included only a small population with uterine carcinomas which included not only cervical carcinoma but also corpus carcinoma. Moreover, the number of patients in whom the therapeutic response to chemoradiotherapy was monitored was also small. Since our study was designed to assess staging prior to surgery, the results from this patient population with uterine carcinoma will not explain the staging accuracy of advanced disease. Long term follow-up is needed as to whether therapeutic response evaluated by ^{11}C-choline PET/CT can accurately reflect prognosis or not. ^{11}C-choline seems to be a sensitive PET tracer for the management of uterine carcinoma. However, the short half-life of ^{11}C-choline is the main cause of practical restriction. ^{18}F-choline has a longer half-life than ^{11}C-choline and has been used to diagnose prostate carcinoma [24, 25]. The sensitivity values may be affected by differences in urinary secretion, because there is no other reason why these differences between ^{18}F-choline and ^{11}C-choline should lead to improved accuracy of PET/CT.

The total numbers of patients were small and heterogeneous, and our present study is retrospective and reflects our initial experience. Further studies involving a larger number of patients and histological correlation are required to determine the clinical usefulness of ^{11}C-choline PET/CT in monitoring the therapeutic response to chemoradiotherapy in patients with cervical carcinoma.

In conclusion, combining ^{11}C-choline PET/CT and MRI increases the accuracy of staging in patients with uterine carcinoma. ^{11}C-choline PET/CT may be feasible as a method of evaluating therapeutic response after chemoradiotherapy in patients with cervical carcinoma. The results demonstrated its advantages and potential in ^{11}C-choline PET/CT, but clinical evaluation in a large patient population is warranted before applying it as an optional approach for the management of uterine carcinoma.

Acknowledgments This work was supported in part by grants from Scientific Research Expenses for Health and Welfare Programs and the Grant-in-Aid for Cancer Research from the Ministry of Health, Labour and Welfare.

References

1. Hara T, Kosaka N, Shinoura N, Kondo T. PET imaging of brain tumor with [methyl-^{11}C]choline. J Nucl Med. 1997;38:842–7.

2. Hara T, Kosaka N, Kishi H. PET imaging of prostate cancer using carbon-11-choline. J Nucl Med. 1998;39:990–5.
3. Jager PL, Que TH, Vaalburg W, Prium J, Elsinga P, Plukker JT. Carbon-11 choline or FDG-PET for staging of oesophageal cancer? Eur J Nucl Med. 2001;28:1845–9.
4. Pieterman RM, Que TH, Elsinga PH, Pruim J, van Putten JW, Willemsen AT, et al. (11)C-choline and (18)F-FDG PET in primary diagnosis and staging of patients with thoracic cancer. J Nucl Med. 2002;43:167–72.
5. de Jong IJ, Prium J, Elsinga PH, Vaalburg W, Mensink HJ. Preoperative staging of pelvic lymph nodes in prostate cancer by 11C-choline PET. J Nucl Med. 2003;44:331–5.
6. Picchio M, Treiber U, Beer AJ, Metz S, Bossner P, van Randenborgh H, et al. Value of 11C-choline PET and contrast-enhanced CT for staging of bladder cancer: correlation with histopathologic findings. J Nucl Med. 2006;47:938–44.
7. Tian M, Zhang H, Oriuchi N, Higuchi T, Endo K. Comparison of ^{11}C-choline PET and FDG PET for the differential diagnosis of malignant tumors. Eur J Nucl Med Mol Imaging. 2004;31:1064–72.
8. Scher B, Seitz M, Albinger W, Tiling R, Scherr M, Becker HC, et al. Value of (11)C-choline PET and PET/CT in patients with suspected prostate cancer. Eur J Nucl Med Mol Imaging. 2007;34:45–53.
9. Torizuka T, Kanno T, Futatsubashi M, Okada H, Yoshikawa E, Nakamura F, et al. Imaging of gynecologic tumors: comparison of ^{11}C-choline PET with ^{18}F-FDG PET. J Nucl Med. 2003; 44:1051–6.
10. Therasse P, Arbuck SG, Eisenhauer EA, Wanders J, Kaplan RS, Rubinstein L, et al. New guidelines to evaluate the response to treatment in solid tumors. European Organization for Research and Treatment of Cancer, National Cancer Institute of the United States, National Cancer Institute of Canada. J Natl Cancer Inst. 2000;92:205–16.
11. Young H, Baum R, Cremerius U, Herholz K, Hoekstra O, Lammertsma AA, et al. Measurement of clinical and subclinical tumour response using [18F]-fluorodeoxyglucose and positron emission tomography: review and 1999 EORTC recommendations. European Organization for Research and Treatment of Cancer (EORTC) PET Study Group. Eur J Cancer. 1999;35: 1773–82.
12. Nakamoto Y, Eisbruch A, Achtyes ED, Sugawara Y, Reynolds KR, Johnston CM, et al. Prognostic value of positron emission tomography using F-18-fluorodeoxyglucose in patients with cervical cancer undergoing radiotherapy. Gynecol Oncol. 2002; 84:289–95.
13. Grigsby PW, Siegel BA, Dehdashti F, Rader J, Zoberi I. Post-therapy [18F] fluorodeoxyglucose positron emission tomography in carcinoma of the cervix: response and outcome. J Clin Oncol. 2004;22:2167–71.
14. Yoshida Y, Kurokawa T, Kawahara K, Yagihara A, Tsuchida T, Okazawa H, et al. Metabolic monitoring of advanced uterine cervical cancer neoadjuvant chemotherapy by using [F-18]-Fluorodeoxyglucose positron emission tómography: preliminary results in three patients. Gynecol Oncol. 2004;95:597–602.
15. Xue F, Lin LL, Dehdashti F, Miller TR, Siegel BA, Grigsby PW. F-18 fluorodeoxyglucose uptake in primary cervical cancer as an indicator of prognosis after radiation therapy. Gynecol Oncol. 2006;101:147–51.
16. Bar-Shalom R, Yefremov N, Guralnik L, Gaitini D, Frenkel A, Kuten A, et al. Clinical performance of PET/CT in evaluation of cancer: additional value for diagnostic imaging and patient management. J Nucl Med. 2003;44:1200–9.
17. Hara T, Yuasa M. Automated synthesis of [^{11}C]choline, a positron-emitting tracer for tumor imaging. Appl Radiat Isot. 1999; 50:531–3.
18. Sobin LH, Wittekind C. UICC TNM classification of malignant tumours. 6th ed. New York: Wiley; 2002.
19. Benedet JL, Bender H, Jones H III, Ngan HY, Pecorelli S. FIGO staging classifications and clinical practice guidelines in the management of gynecologic cancers. FIGO Committee on Gynecologic Oncology. Int J Gynaecol Obstet. 2000;70:209–62.
20. Togashi K, Nishimura K, Sagoh T, Minami S, Noma S, Fujisawa I, et al. Carcinoma of the cervix: staging with MR imaging. Radiology. 1989;171:245–51.
21. Manfredi R, Mirk P, Maresca G, Margariti PA, Testa A, Zannoni GF, et al. Local-regional staging of endometrial carcinoma: role of MR imaging in surgical planning. Radiology. 2004;231:372–8.
22. Grigsby PW, Siegel BA, Dehdashti F. Lymph node staging by positron emission tomography in patients with carcinoma of the cervix. J Clin Oncol. 2001;19:3745–9.
23. Sironi S, Buda A, Picchio M, Perego P, Moreni R, Pelleqrino A, et al. Lymph node metastasis in patients with clinical early-stage cervical cancer: detection with integrated FDG PET/CT. Radiology. 2006;238:272–9.
24. Heinisch M, Dirisamer A, Loidl W, Stoiber F, Gruy B, Haim S, et al. Positron emission tomography/computed tomography with F-18-fluorocholine for restaging of prostate cancer patients: meaningful at PSA <5 ng/ml? Mol Imaging Biol. 2006;8:43–8.
25. Gutman F, Aflalo-Hazan V, Kerrou K, Montravers F, Grahek D, Talbot JN. 18F-choline PET/CT for initial staging of advanced prostate cancer. AJR Am J Roentogenol. 2006;187:618–21.

Surg Today (2009) 39:144–147
DOI 10.1007/s00595-008-3811-x

SURGERY TODAY

Middle-Colic Artery Aneurysm Associated with Segmental Arterial Mediolysis, Successfully Managed by Transcatheter Arterial Embolization: Report of a Case

TAKAHISA HIROKAWA[1,3], HIROZUMI SAWAI[1], KOJI YAMADA[1], TAKEHIRO WAKASUGI[1], HIROMITSU TAKEYAMA[1], HIROYUKI OGINO[2], MASAKATSU TSURUSAKI[3], and YASUAKI ARAI[3]

Departments of [1]Gastroenterological Surgery and [2]Radiology, Nagoya City University Graduate School of Medical Sciences, Nagoya, Japan
[3]Department of Diagnostic Radiology, National Cancer Center Hospital, 5-1-1 Tsukiji, Chuo-ku, Tokyo 104-0045, Japan

Abstract
An aneurysm of the middle-colic artery, associated with segmental arterial mediolysis (SAM), is a rare condition. This report describes a case of a middle-colic artery aneurysm that was associated with SAM. A 57-year-old man was admitted to our hospital because of severe abdominal pain. A rupture of a middle-colic artery aneurysm was diagnosed by computed tomography, and angiography showed that it may have been associated with SAM. The ruptured aneurysm was successfully treated with transcatheter arterial embolization. Transcatheter arterial embolization might be one of the best treatments for such a complicated aneurysm occurring in a visceral artery.

Key words Middle-colic artery aneurysm · Segmental arterial mediolysis · Transcatheter arterial embolization

Introduction

The most frequent site of a visceral artery aneurysm is the splenic artery, but it is a rare occurrence. Therefore, an aneurysm of the middle-colic artery is even more uncommon.[1] An aneurysm that may be caused by segmental arterial mediolysis (SAM) is also a rare condition. This report documents a case of a SAM-associated, ruptured, middle-colic artery aneurysm that was successfully managed by transcatheter arterial embolization (TAE).

Reprint requests to: T. Hirokawa (address 3)
Received: February 25, 2008 / Accepted: May 14, 2008

Case Report

A 57-year-old man with no previous medical history was admitted to a local hospital because of severe abdominal pain and diarrhea. Contrast-enhanced computed tomography (CT) showed ascites throughout the abdomen and higher CT-value ascites rather than serous ascites in the upper abdomen. Abdominocentesis revealed the presence of hemoperitoneum. Angiography located the aneurysm within the left branch of middle-colic artery, but no extravagation was seen. The CT scan revealed a hematoma around the transverse mesocolon (Fig. 1) indicating a rupture of this aneurysm. Therefore the patient was transferred to this hospital. When he arrived, his vital signs included a low grade fever (37.5°C), hypertension (184/86 mmHg), and a slight tachycardia (102 beats/min). He was not pale and had clear consciousness. A physical examination revealed only slight abdominal tenderness. The laboratory findings showed anemia (red blood cell count: 2.5 million/μl; hemoglobin: 8.4 g/dl; hematocrit: 24.3%) and inflammation (white blood cell count: 7200/μl, C-reactive protein: 4.58 mg/dl).

Angiography detected a middle-colic artery aneurysm, a wide and narrow irregularity in the distal artery of the aneurysm, but no extravagation (Fig. 2a). The results also indicated that this aneurysm was ruptured and it had a risk of further bleeding. Transcatheter arterial embolization was applied initially because it was less invasive treatment than surgery. Using a right femoral artery approach, a 4-Fr C2 catheter (Clinical Supply, Hashima, Japan) was placed in the superior mesenteric artery, and the proximal middle-colic artery was selected with micro-catheter (Renegade; Boston Scientific Japan, Tokyo, Japan). However, because of the meandering of the middle-colic artery, the microcatheter could not be inserted at the aneurysm. Therefore, microcoils could not be used. Then approximately 0.3 ml of iodized oil (Lipiodol) mixed with *N*-butyl-2-

cyanoacrylate (NBCA) (Lipiodol:NBCA = 3:2) was injected into the root of the distal branch via the aneurysm. Postembolization angiography demonstrated no filling of the aneurysm. On delayed images, the distal arteries of the aneurysm were barely evident, thus the risk of ischemic colitis was low (Fig. 2b), and surgical treatment was avoided. In addition, further arterial examinations were conducted. Celiac angiography revealed two other aneurysms. One was at the root of the celiac artery and the other at the left hepatic artery. Inferior mesenteric arterial angiography found no aneurysm, but a wide and narrow irregularity was seen. These observations suggested that these abnormal angiographic findings and aneurysms might therefore be related to SAM.

The patient's post-TAE course was uneventful and his anemia improved. A contrast-enhanced CT scan obtained 2 days later showed that the size of the hematoma had decreased and the aneurysm had been embolized (Fig. 3). The patient was discharged 1 week after TAE. Colonoscopy 3 months later showed no evidence of bowel ischemia, and he is currently doing well without symptoms.

Discussion

Visceral aneurysms are relatively rare. The most common sites of visceral arterial aneurysms are the splenic artery (60%), hepatic artery (20%), superior mesenteric artery (5.5%), celiac artery, gastric and gastroepiploic arteries (4%), and jejunal, ileal, and colonic arteries and their tributaries (3%).[1] Aneurysms of the superior mesenteric arterial branch, particularly the middle-colic artery, are very uncommon. These are generally asymptomatic and are usually found incidentally.

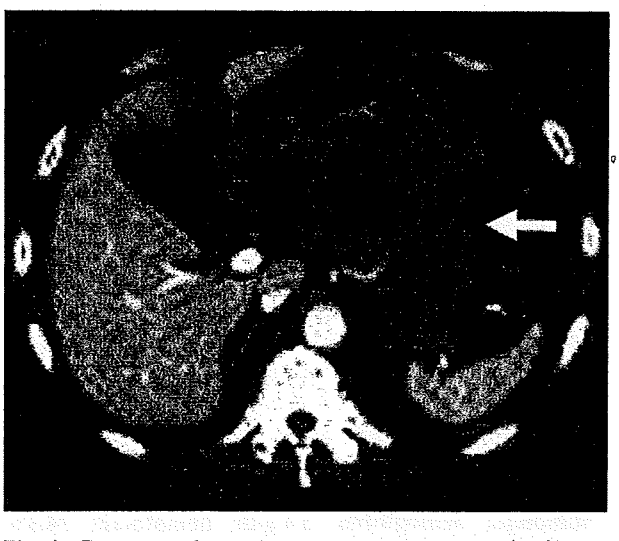

Fig. 1. Contrast-enhanced computed tomography (CT) scan shows extensive ascites in the omental bursa and around the transverse mesocolon (*arrow*)

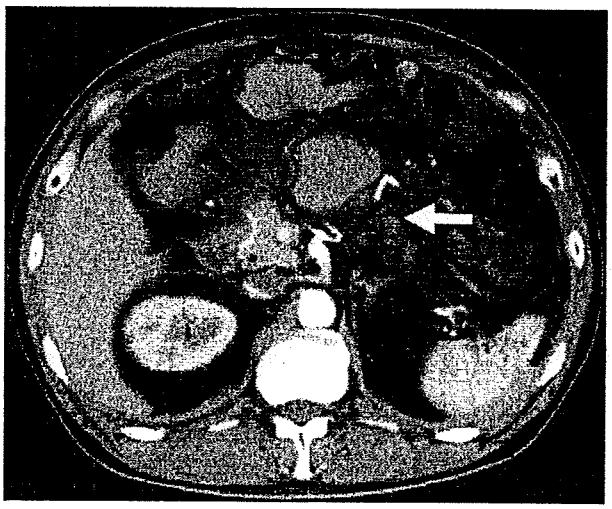

Fig. 3. The successful embolization of the aneurysm of the middle-colic artery is shown on contrast-enhanced CT scan at 2 days after TAE (*arrow*)

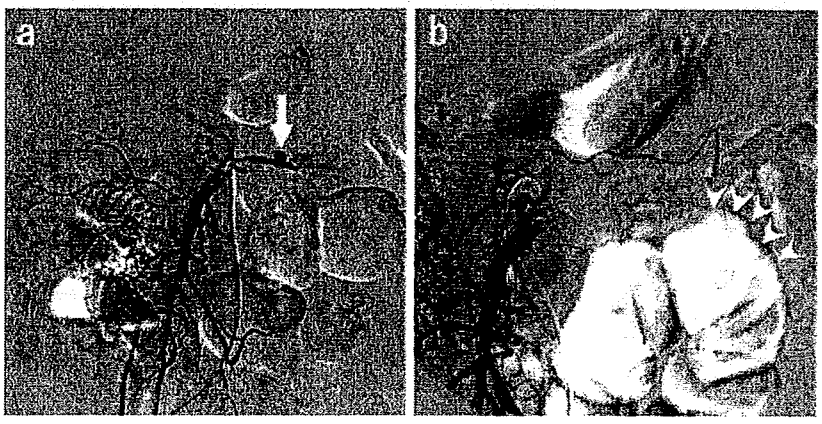

Fig. 2. a Angiography of the superior mesenteric artery shows that the aneurysm is in the left branch of middle-colic artery (*arrow*), but no extravasations are seen. **b** The left branch of the middle-colic artery was successfully embolized by transcatheter arterial embolization (TAE); there is no filling of the aneurysm. On delayed images, the distal arteries of the aneurysm are barely evident, indicating that the risk of ischemic colitis was low (*arrowheads*)

Table 1. Cases of middle colic artery aneurysms (7 cases after Sarcina et al.[2] reviewed in 2000)

First author[Ref.]	Year	Age (years)	Sex	Chief symptoms	Past history/ present illness	Diagnosis	Treatment	Other aneurysms
LaBerge[3]	1999	52	M	Abdominal pain, nausea, vomiting	Hypertension	Angiography	Resection	Yes
Sarcina[2]	2000	72	F	Dyspepsia, epigastric discomfort	Hypertension	Angiography	Resection	No
Matsuo[4]	2001	68	M	Anemia	Not described	Angiography	Resection	Not described
Sato[5]	2001	68	M	Abdominal pain	None	Surgery	Resection	No
Toyonaga[6]	2002	73	M	Abdominal pain, vomiting	Acute pancreatitis	Angiography	Embolization	No
Chino[7]	2004	78	M	Abdominal pain, nausea	Renal stones, gout	Surgery	Bowel-resection	No
Present case		57	M	Abdominal pain	None	Angiography	Embolization	Yes

Sarcina et al.[2] reviewed the literature of the 28 cases of middle-colic artery aneurysms reported between 1937 and 1995, and Medline was searched using the keywords "Middle-colic artery" and "aneurysm," and another 5 cases of middle-colic artery aneurysm were found (Table 1).[2–7] The data from the 35 reported cases, including the current case, were analyzed. The mean age and age range were 59.3 ± 13.3 years and 19–78 years, respectively. The ratio of males to females was 19:16; thus, there appears to be no significant gender difference. In almost all cases, the chief complaint was abdominal pain. In total, 45.7% of the cases (16/35) had multiple aneurysms. Most cases were treated surgically. An aneurysm ligation was performed in 11 cases, resection was performed in 8 cases, and a bowel resection was required in 9 cases. Transcatheter arterial embolization was chosen in only 3 cases. Embolization was performed using particles of gelatin sponge inserted in one case,[8] using microcoils in one case,[6] and in the present case, a mixed emulsion of Lipiodol and NBCA was used. Using this embolic agent, it was possible to embolize the aneurysm root and its proximal and distal feeders in one step. However, this procedure is associated with risks including bowel ischemia, and aneurysm rupture using this agent for the treatment of lower bowel hemorrhage or aneurysm is still controversial. Most mesenteric artery embolizations are performed using microcoils.[9] But in the present case, NBCA was used with Lipiodol because distal catheterization of the aneurysm could not be achieved. NBCA is a liquid embolic agent whose time to coagulation after injection can be controlled by diluting it with Lipiodol. It might be possible to embolize an aneurysm, feeding vessels, and efferent vessels using an NBCA–Lipiodol mixture of an appropriate concentration, even if the catheter cannot reach the aneurysm. The aneurysm in the present case was successfully embolized using this method.

Tulsyan et al.[10] studied 90 cases of visceral artery aneurysms and pseudoaneurysms and found that endovascular treatment was technically successful in 98% of the cases. In the review of 9 cases of visceral artery aneurysm by Kasirajan et al.,[11] aneurysm exclusion was achieved in 75% cases by coil embolization. They concluded that percutaneous transcatheter coil embolotherapy is an effective alternative to open surgery and that therapy may decrease the morbidity and mortality associated with open surgical procedures. There have been very few reported cases of NBCA embolization for visceral artery, but there are no reports of complications including ischemia.[12] This report suggested the embolization with NBCA is a safe method. Above all, because this endovascular method is at least as safe as open surgery and less invasive, it is one of the best treatments for a visceral artery aneurysm.

The association of the aneurysms in this case to SAM was indicated by the presence of multiple aneurysms and luminal irregularities of the artery walls. The pathogenesis of SAM is poorly understood and was first described by Slavin and Gonzalez-Vitale in 1976, and at first the name "segmental mediolytic arteritis (SMA)" was coined.[13] They described unique vascular lesions, so-called mediolytic lesions, in three autopsy cases of SMA, which were characterized by lytic degeneration of the arterial media. Based on their later observations, together with the inconstant association of inflammation in the involved arteries and the general absence of clinical and laboratory evidence of vasculitis, the term SMA was changed to "segmental arterial mediolysis (SAM)" in 1995.[14] From this etiology, this disease is also called "segmental mediolytic arteriopathy," but now the name "SAM" is the most frequently used. According to a review of 20 cases of SAM involving abdominal splanchnic arteries by Takagi et al.,[15] SMA occurs in middle-aged to elderly people (range, 39–87 years) of

both sexes, usually involves more than one visceral artery, and most frequently, branches of the celiac axis. The current case was compatible with these cases. Generally the visceral aneurysms are related to an infection represented by subacute bacterial endocarditis, polyarteritis nodosa, and others. In the present case, there had been no previous infectious disease. Following the TAE, the patient is doing well and there have been no signs of inflammation, and thus no need for any steroid or immunosuppressive drug therapies. One limitation to this study is that no pathological examination was carried out, but the clinical and radiographical findings strongly suggested SAM. In conclusion, this was a rare case of a ruptured middle-colic artery aneurysm associated with SMA, which is the first case to be treated by Lipiodol and NBCA embolization.

References

1. Moore WS. Vascular surgery: a comprehensive review. 3rd ed. Philadelphia, PA: Saunders; 1991.
2. Sarcina A, Bellosta R, Magnaldi S, Luzzani L. Aneurysm of the middle colic artery — case report and literature review. Eur J Vasc Endovasc Surg 2000;20:198–200.
3. LaBerge K. SCVIR Annual Meeting film panel session: case 3. JVIR 1999;10:509–13.
4. Matsuo S, Yamaguchi S, Miyamoto S, Ishii T, Tsuneoka N, Obata S, et al. Ruptured aneurysm of the visceral artery: report of two cases. Surg Today 2001. 31:660–4.
5. Sato T, Itoh M, Ohta N, Funaki H, Saito Z, Takayanagi N. Spontaneous ruptured middle colic artery aneurysm with concurrent renal cell carcinoma. Hepato-Gastroenterology 2001;48: 678–80.
6. Toyonaga T, Nagaoka S, Ouchida K, Nagata M, Shirota T, Ogawa T, et al. Case of a bleeding pseudoaneurysm of the middle colic artery complicating acute pancreatitis. Hepato-Gastroenterology 2002;49:1141–3.
7. Chino O, Kijima H, Shivuya M, Yamamoto S, Kashiwagi H, Kondo Y, et al. A case report: spontaneous rupture of dissecting aneurysm of the middle colic artery. Tokai J Exp Clin Med 2004;29:155–8.
8. Naito A, Toyota N, Ito K. Embolization of a ruptured middle colic artery aneurysm. Cardiovasc Intervent Radiol 1995;18: 56–8.
9. d'Othee BJ, Surapaneni P, Rabkin D, Nasser I, Clouse M. Microcoil embolization for acute lower gastrointestinal bleeding. Cardiovasc Intervent Radiol 2006;29:49–58.
10. Tulsyan N, Kashyap VS, Greenberg RK, Sarac TP, Clair DG, Pierce G, et al. The endovascular management of visceral artery aneurysms and pseudoaneurysms. J Vasc Surg 2006;45:276–83.
11. Kasirajan K, Greenberg RK, Clair D, Ouriel K. Endovascular management of visceral artery aneurysm. J Endovasc Ther 2001;8:150–5.
12. Kish JW, Katz MD, Marx MV, Harrell DS, Hanks SE. N-butyl cyanoacrylate embolization for control of acute arterial hemorrhage. J Vasc Interv Radiol 2004;15:689–95.
13. Slavin RE, Gonzalez-Vitale JC. Segmental mediolytic arteritis. A clinical pathologic study. Lab Interv 1976;35:23–9.
14. Slavin RE, Saeki K, Bhagavan B, Maas AE. Segmental arterial mediolysis: a precursor to fibromuscular dysplasia?. Mod Pathol 1995;8:287–94.
15. Takagi C, Ashizawa N, Eishi K, Ashizawa K, Hayashi T, Tanaka K, et al. Segmental mediolytic arteriopathy involving celiac to splenic and left renal arteries. Intern Med 2003;42:818–23.

original article

Annals of Oncology 20: 1943–1947, 2009
doi:10.1093/annonc/mdp242
Published online 1 July 2009

Phase I/II clinical study of percutaneous vertebroplasty (PVP) as palliation for painful malignant vertebral compression fractures (PMVCF): JIVROSG-0202

T. Kobayashi[1]*, Y. Arai[2], Y. Takeuchi[2], Y. Nakajima[3], Y. Shioyama[4], M. Sone[5], N. Tanigawa[6], O. Matsui[7], M. Kadoya[8] & Y. Inaba[9] Japan Interventional Radiology in Oncology Study Group (JIVROSG)

[1]*Department of Diagnostic and Interventional Radiology, Ishikawa Prefectual Central Hospital, Ishikawa;* [2]*Department of Diagnostic Radiology Division, National Cancer Center Hospital, Tokyo;* [3]*Department of Radiology, St. Marianna University, Yokohama;* [4]*Department of Radiology, Dokkyo Medical University, Tochigi;* [5]*Department of Radiology, Iwate Medical University, Iwate;* [6]*Department of Radiology, Kansai Medical University, Isaka;* [7]*Department of Radiology, Kanazawa University, Ishikawa;* [8]*Department of Radiology, Shinshu University, Matsumoto and* [9]*Department of Diagnostic and Interventional Radiology, Aichi Cancer Center, Aichi, Japan*

Received 8 May 2008; revised 18 November 2008; revised 18 March 2009; accepted 26 March 2009

Background: The safety and efficacy of percutaneous vertebroplasty (PVP), a new treatment modality for painful malignant vertebral compression fractures (PMVCF) using interventional radiology techniques, were evaluated prospectively.
Materials and methods: After confirming the absence of safety issues in phase 1, a total of 33 cases were registered up to and including phase 2. Safety and efficacy were evaluated by National Cancer Institute—Common Toxicity Criteria version 2 and Visual Analogue Scale (VAS) at 1 week after PVP. Based on VAS score decreases, efficacy was classified into significantly effective (SE; ≥5 or reached 0–2), moderately effective (ME; 2–4), or ineffective (NE; <2 or increase).
Results: Procedures were completed in all 33 patients (42 vertebrae). Thirty days after PVP, two patients died of primary disease progression, but no major adverse reactions (>grade 2) were observed. Response rate was 70% (95% confidence interval 54% to 83%) [61% (n = 20) with SE, 9% (n = 3) with ME, and 30% (n = 10) with NE] and increased to 83% at week 4. Median time to response was 1 day (mean 2.4). Median pain-mitigated survival period was 73 days.
Conclusion: For PMVCF, PVP is a safe and effective treatment modality with immediate onset of action.
Key words: percutaneous vertebroplasty, interventional radiology, pain relief, vertebral metastasis, percutaneous cement plasty

introduction

The pain relief of painful malignant vertebral compression fractures (PMVCF) is one of the key elements for achieving better quality of life in patients under palliative care. The mainstay for pain relief is pharmacological therapy such as with nonsteroidal anti-inflammatory drugs (NSAIDs) and opioids, and if patients are not responsive to these agents or have pain upon body movement, radiotherapy is administered. However, despite being a noninvasive therapeutic modality, radiotherapy is less than ideal because it requires 2–4 weeks to obtain a therapeutic effect and does not achieve complete pain relief in most cases [1, 2].

Since the report of percutaneous vertebroplasty (PVP) by Galibert et al. [3], in 1987, the technique has been widely reported [4–10]. These reports indicate that it is highly effective for prompt pain relief for metastatic vertebral tumors from any primary sites. On the other hand, severe, albeit rare, complications such as pulmonary embolism, cerebral infarction, cardiogenic shock, and spinal cord injury due to leakage of cement into the spinal canal have also been documented [11–13]. All these reports, however, have been retrospective in nature, and to our knowledge, no study has yet prospectively investigated the safety and therapeutic effect of this modality. Although it cannot be excluded that severe complications may very rarely occur, to minimize the frequency of reported complications, it is important to evaluate in a prospective study whether this procedure can be carried out safely when conducted by trained interventional radiologists for clearly defined indications.

Therefore, we undertook a phase I/II multi-institutional prospective study of PVP as Japan Interventional Radiology in Oncology Study Group (JIVROSG)-0202. In this study, we evaluated the safety and efficacy of PVP as a palliative intervention for patients with PMVCF.

materials and methods

patient selection

Patients were required to have an imaging [including radiography and computed tomography (CT)] diagnosis of changes in the thoracic or

Correspondence to: Dr T. Kobayashi, Department of Diagnostic and Interventional Radiology, Ishikawa Prefectual Central Hospital, Kuratsukihigashi 2-1, Kanazawa-shi, Ishikawa Prefecture, 920-8530, Japan. Tel: +81-76-237-8211; Fax: +81-76-238-2337; E-mail: kobaken@ipch.jp

lumbar vertebrae caused by malignant tumor metastases or multiple myeloma, limitation of daily activities due to pain from the lesions and/or the risk of compression fracture, and no exposure of the vertebral tumors to the vertebral canal (defined as vertebral canal surface showing no tumor invasion on CT or magnetic resonance imaging). In addition, the patients had to have an Eastern Cooperative Oncology Group performance status (PS) of zero to three, preserved major organ function (bone marrow, heart, liver, lung, and kidney), and an anticipated survival of at least 4 weeks. Patients were excluded if their pain grade of Visual Analogue Scale (VAS) [14] was ≤2, they could not maintain the position needed for treatment, they had a bleeding tendency with bleeding time ≥5 min, fever ≥38°C, cardiac failure requiring continuous drug therapy, history of major drug allergy such as anaphylactic shock to any drugs, so as to minimize the possibility of cardiac toxicity due to the bone cement preparation, and/or confirmed or possible pregnancy. In addition, patients were judged ineligible for this trial if the vertebral lesions harbored possible active inflammation (tuberculous or other infectious), if marked vertebral flattening was present (defined as the height of the affected vertebral body showing a mean value of one-third of that of the superior and inferior vertebral bodies), if five or more continuous vertebrae were affected precluding evaluation of the therapeutic effect or if in a single session four or more vertebrae required therapy.

Both the ethics committee of the Japanese Society of Interventional Radiology and each institutional review board approved the protocol of this study before patient entry. All patients provided written informed consent.

collaborative institutions

This study was conducted in 10 institutions comprising JIVROSG. Each of these institutions has at least one full-time interventional radiologist certified by the Japanese Society of Interventional Radiology (Table 1).

study end points

The primary end point of this study was to evaluate the safety of PVP, and the secondary end point was to evaluate the efficacy of PVP for pain relief as well as the incidence and grade of adverse events.

study design

This study was a multi-institutional, single-arm, open-label, noncomparative trial. The phase I part of this trial was conducted using the 3 × 3 method proposed by the JIVROSG. This method was applied as follows. To be able to quickly terminate the study if the incidence of adverse events associated with this modality exceeded one-third of the patients, three separate groups with three cases each were enrolled at 4-week intervals. If severe adverse events of the first group with three cases, according to the National Cancer Institute—Common Toxicity Criteria (NCI-CTC) version 2.0 [15] or equivalent adverse events, were limited to one or less of the first three cases, then the second group with three cases was added. When the number of adverse events in the combined first and second groups with six cases was two or less, then the third group with three cases was added. If the number of adverse events of the total nine cases of all three groups was three or less, then subsequently all cases up to the target number were enrolled without distinguishing them into three different groups. If the incidence of adverse events in each of the first, second and third groups exceeded the above-noted permissible limits, the advisability of trial continuation or possible termination was rediscussed.

Table 1. Collaborative institutions

National Cancer Center Hospital
Kyoto First Red Cross Hospital
St Marianna University
Ibaraki Prefectural Central Hospital
Kansai Medical University
Iwate Medical University
Kanazawa University
Shinshu University
Aichi Cancer Center
Tochigi Cancer Center Hospital

In the phase II part of this study, 24 cases were enrolled. Since the treatment administered in phases 1 and 2 was exactly the same, the primary and secondary end points of the cases registered in phase 1 were evaluated together with those of the cases of phase 2. So, the primary and secondary end points were evaluated in all 33 cases.

The observation period for adverse events was defined as the 1-month period following the completion of the procedure. Subsequently, the presence/absence of pain recurrence at the treated site, the period of pain relief (absence of recurrent pain at the treated site from before therapy to obtaining a decrease of VAS score to ≤2), and patient survival period were investigated. In the follow-up investigation, recurrence was defined as occurring on the day on which pain worse than that before therapy was noted, with the period up to this day defined as the pain-mitigated survival period.

statistical analysis

In the phase I part of this study, a cohort size of nine patients was considered to make it possible to quickly terminate the study if the incidence of adverse events associated with this modality exceeded one-third. During phase I through phase II, the study was designed to detect adverse events having an incidence of at least 10%, setting 80% power, 10% predicted rate, and 30% unacceptable rate. We anticipated a protocol dropout rate of 10%. Thus, the target accrual number of patients was calculated to be 33. All enrolled patients were included for the intention-to-treat analyses.

registration of cases

The registration period extended from February 2003 until May 2006. To enter a patient into the study, the investigator had to log on to a restricted Web site using the JIVROSG data center, enter patient indication/contraindication data, and register the case. After the executive office verified the suitability of the entered data and the presence/absence of any missing items, a registration number specific to that patient was issued and the case registration procedure completed. Subsequently, all communications were limited to these issued patient registration numbers. PVP was commenced within 1 week of this patient registration.

interventional procedures of PVP

The interventional procedures of PVP in this study were conducted as follows. After injection of 0.5 mg atropine sulfate and securing a venous access, the patient was placed prone on the table used for fluoroscopy or CT fluoroscopy, and an electrocardiogram apparatus and blood pressure monitor were attached. Following disinfection of the puncture site and injection of local anesthesia, an 11–14 ga metallic needle was inserted up to the site where the bone cement was to be injected under fluoroscopic or CT-fluoroscopic guidance (Figure 1A). Acrylic bone cement was prepared, and the use of bone cement mixed with up to 30% bactericidal barium was recommended if bone cement was injected under fluoroscopic guidance (Figure 1B). The injection was stopped when sufficient bone cement was judged to have been distributed, after which the needle was withdrawn (Figure 1C). When multiple (up to three) vertebrae were to be treated, these steps were repeated for each vertebra. The patient was kept at bed rest for 2 h after the procedure.

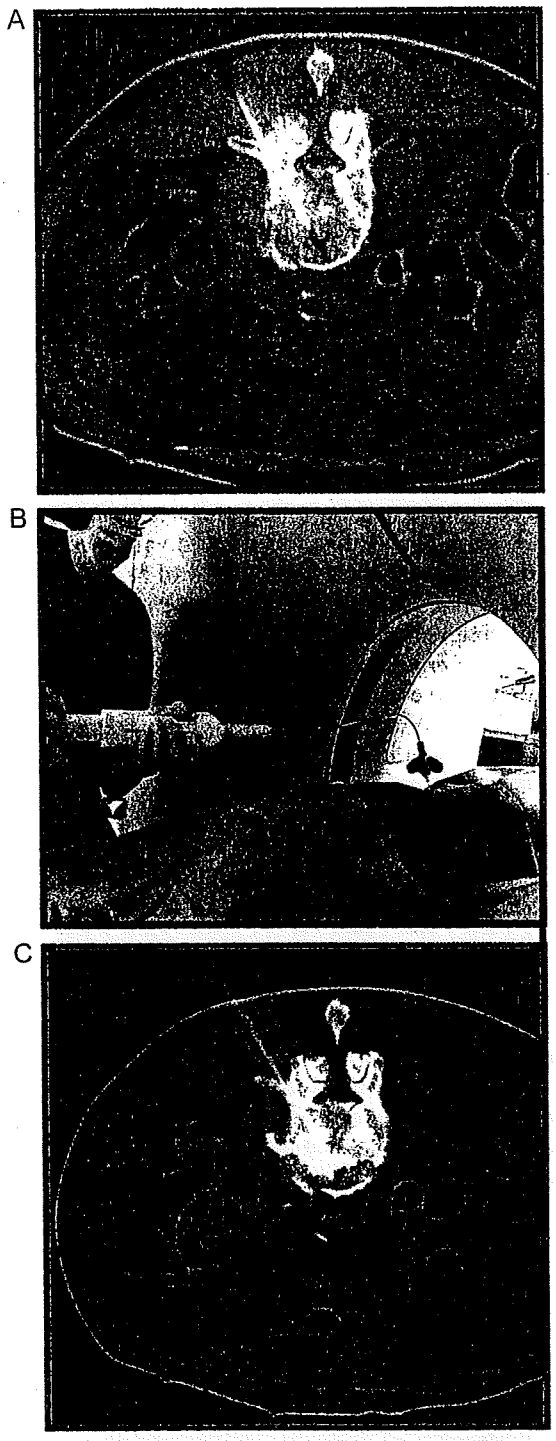

Figure 1. Interventional procedure of percutaneous vertebroplasty. (A) Insertion of 11–14 ga bone biopsy needle into the target vertebral bone through pedicle under fluoroscopic or computed tomography (CT)-fluoroscopic guidance. (B) Injection of acrylic bone cement under fluoroscopy or CT fluoroscopy monitoring. (C) Stop of the injection when adequate distribution is obtained.

combined and supportive therapies

To prevent possible infection, it is recommended that antibiotics be administered for 3 days following the procedure and that an anesthesiologist or other physician able to undertake emergency measures be present. Continued administration of any radiotherapy or analgesics, chemotherapy, and nerve block therapy used before therapy was permitted, including the wearing of corsets. With the exception of management of adverse events, surgical intervention for post-therapy pain, admixture of anticancer agents and/or antibiotics with the acrylic bone cement, and PVP using general anesthesia were not permitted.

observation items

The imaging findings including those of radiography and CT of the primary site and target vertebrae and compression grade were evaluated before therapy and at around 7 days after therapy. VAS score was determined at days 1, 3, and 7 and weeks 2 and 4. Also, before and after therapy, the patient items were evaluated at the specified times.

evaluation methods

The adverse events were evaluated by NCI-CTC version 2. The grade of pain was evaluated by the VAS. VAS scoring was done by having the patient himself note his degree of pain on a 10-cm long horizontal straight line. The efficacy of therapy was evaluated by changes in the VAS score noted 1 week after therapy. When the VAS score was ≤2 or when compared with before therapy a decrease of ≥5 was obtained, the therapy was judged to be significantly effective (SE). When the VAS score did not reach ≤2 but when compared with before therapy showed a decrease to <5 to ≥2, the therapy was judged to be moderately effective (ME). When despite therapy the VAS score decreased by <2 or showed an increase, the therapy was judged to be ineffective (NE). The efficacy of the therapeutic results was assessed by the proportion of the total cases achieving SE or ME. Regardless of any changes in the VAS score, the therapy was also judged to be NE if the need for analgesics increased as compared with before therapy. However, to investigate the timing of the pain-mitigating effect, VAS score was determined within 1 week before the start of therapy, the day after, 3 days after, and at 1, 2, 3, and 4 weeks.

In cases with painful bone metastases at multiple sites, treatment was permitted for all sites with indications for PVP at multiple sessions. However, one treatment session was limited to a maximum of three vertebrae. When all treatment sessions were finished, the degree of back pain was comprehensively evaluated by VAS.

results

There were no reports of severe adverse event in any of the nine cases enrolled in phase I. Thus, without any interruption the transition was made to phase II. There were a total of 33 cases from 10 institutions, comprising 16 males and 17 females with a mean age of 62 years (37–87 years) (Table 2). PS was zero in one case, one in seven cases, two in 12 cases, and three in 13 cases. Thirty cases had metastatic vertebral tumors, originating from lung, breast, and colon cancer in seven cases each, liver cancer in four cases, pancreas cancer in two cases, and tongue, esophagus, and skin cancer in one case each. The only primary vertebral tumor was multiple myeloma, which was present in three cases. Analgesics administered before therapy were NSAIDs alone in nine cases, opioids alone in 10, and both in 11. Radiotherapy was administered to the treated site in 11 cases. The mean interval between the two therapies was 46 days, and no pain-mitigating effect was obtained.

Forty-two vertebrae were targeted: 18 thoracic vertebrae (I, one; VII, three; VIII, three; IX, four; X, two; XI, two; and XII, three) and 24 lumbar vertebrae (I, one; II, seven; III, seven; IV, seven; and V, two). Changes in imaging findings at the treated sites comprised osteolytic changes in 35 vertebrae, mixed

changes in five vertebrae, and osteoblastic changes in two vertebrae, with the mean compression rate amounting to 75.8% (41%–106%). Three vertebral bodies, two vertebral bodies, and one vertebral body were treated in two, five, and 26 cases, respectively. In only a single case was the treatment divided into two sessions, being completed in a single session in all the other cases.

Table 2. Background of enrolled cases

Patient characteristics	
No. of patients	33[a]
Male	16
Female	17
Mean age, years	62 (37–87)
Primary disease	
Lung cancer	7
Breast cancer	7
Colorectal cancer	7
Liver cancer	4
Myeloma	3
Pancreatic cancer	2
Tongue cancer	1
Esophageal cancer	1
Skin cancer	1
Preradiotherapy to the target lesion	11 (mean interval 46 days)
Combined chemotherapy	16
Administered analgesics before therapy	
NSAIDs alone	9
Opioids alone	10
NSAIDs and opioids	11
Performance status (ECOG)	
0	1
1	7
2	12
3	13
Target VB (N = 42)	
1 VB	26
2 VBs	5
3 VBs	2
Thoracic VB (N = 18)	
I	1
VII	3
VIII	3
IX	4
X	2
XI	2
XII	3
Lumbar VB (N = 24)	
I	1
II	7
III	7
IV	7
V	2
Appearance of lesion	
Osteolytic	28 (35 VBs)
Mixed	3 (5 VBs)
Osteoblastic	2 (2 VBs)
Compression rate (height of target VB/height of next VB)	
Mean	75.8% (41%–106%)

[a]Nine for phase I and 24 for phase II.
NSAIDs, nonsteroidal anti-inflammatory drugs; ECOG, Eastern Cooperative Oncology Group; VB, vertebral bone.

CT fluoroscopy was used in 15 cases, fluoroscopy in 15, and a combination of the two in three. The mean time required per case and per vertebra was 49 min (20–120 min) and 39 min, respectively. The volume of bone cement administered was 1–8 ml [mean 3.5 ml, standard deviation (SD) 1.8 ml]. The bone cement preparations used were Osteobond (Zimmer, IN) in 22 cases, Simplex (Stryker, MI) in 10, and Bone Cement (Zimmer) in one. The recommended antibiotics were used in 19 of 33 cases (58%). The technical success rate was 100%, and in no cases were the interventional procedures provided by the protocol terminated prematurely.

In the evaluation of safety, adverse events during the therapy were limited to bleeding from the puncture site in a single case (3%), in which the bleeding was stopped with 5-min manual pressure. Adverse events of grade 3 or 4 of NCI-CTC version 2 or other correspondingly severe adverse events related to PVP were not observed, while two patient deaths caused by the progression of primary disease were observed within 30 days of PVP. An adverse event of PVP could not be excluded in only a single case (3%) with grade 2 serum hypoalbuminemia.

In the evaluation of clinical efficacy, the response rate was 70% (95% confidence interval 54% to 83%), being SE in 20 cases (61%) and ME in three (9%). The mean time to response was 2.4 days (median 1 day, SD 3.2 days). VAS score was 6.2 + 2.1 within 1 week before the start of therapy, 3.6 + 2.6 the day after, 2.5 + 2.6 after 3 days, and 2.4 + 2.3 at 1 week (5–8 days), 2.3 + 2.7 at 2 weeks (11–15 days), 2.0 + 2.2 at 3 weeks (15–26 days), and 1.8 + 2.3 at 4 weeks (26–29 days) (Figure 2).

Pain recurrence at the treated site was noted in 5 of 23 (22%) of the SE or ME cases. On the other hand, in 4 of the 10 cases (40%) in which the therapy was evaluated as ineffective in the first week, the result was subsequently judged to be ME. At 4 months after completion of enrollment, 14 patients were alive, 18 had died, and the survival status of one was unknown. The median survival period was 194 days (mean 270 days, SD 240

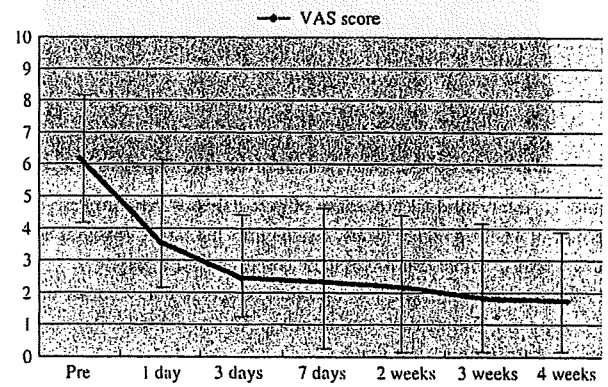

Figure 2. Changes in Visual Analogue Scale (VAS) score. The changes in the VAS values at the various observation time points are listed here. The curve shows the changes in mean values and the vertical line the standard deviation. Pain relief from the therapy is obtained by the third day, with a slow decrease in the VAS values also subsequently observed.

days). The median pain-mitigated survival period was 73 days (mean 230 days, SD 258 days).

discussion

The treatment of painful vertebral metastases and other conditions affecting vertebral bone remains a major challenge in patients under palliative care. Numerous studies have already validated the efficacy and safety of PVP in this context [4–7, 11]. However, all these were retrospective in nature, and no such prospective studies have yet been described. This prompted JIVROSG to undertake the present study to objectively evaluate this procedure by prospectively assessing its safety and clinical efficacy in a multi-institutional setting.

Regarding safety, we attributed the absence of severe complications in the present study to the strict patient selection criteria adopted by us, namely, the exclusion of cases with cardiac failure, a history of drug allergy, and tumors exposed within the vertebral canal, as well as the use of a highly precise fluoroscopy or CT fluoroscopy apparatus at the time of therapy, and the use during fluoroscopy of bone cement mixed with up to 30% bactericidal barium so as to facilitate the immediate recognition of extravertebral leakage. These results indicate that PVP is an extremely safe therapeutic intervention, provided that appropriate patient selection and apparatus use are adhered to, when carried out by an interventional radiology specialist.

In this study, pain was evaluated at 1 week after therapy, with an efficacy rate of 70% obtained, comparable to previously reported results of 70%–90% in the literature [4, 7, 10, 11]. However, most importantly, the therapeutic effect was apparent at a median 1 day (mean 2.4 days, SD 3.2 days), demonstrating a rapid pain-relieving effect. In contrast, the therapeutic response to the hitherto standard pain relief therapeutic modality used, namely, 10 sessions of radiotherapy at 3 Gy, has been reported to require 2–4 weeks to take effect [1, 2]. In this respect, thus, the rapidity of onset of the desired effect of PVP is clearly superior to that of radiotherapy. The median survival period of the enrolled cases was 194 days because ≥90 of them had bone metastases from malignant tumors and had a poor prognosis. In view of this fact, the selection of a therapeutic modality providing a prompt onset of pain relief becomes especially important. In contrast, in cases with vertebral body metastases highly sensitive to radiotherapy and/or with an anticipated long survival period, radiotherapy is the preferred option.

Recurrence of pain at the treated site was noted in 21% of cases. Since this therapy is not designed to exert an antitumor effect but rather to provide pain relief by strengthening weakened vertebrae, pain recurrence is unavoidable if the metastatic foci expand. The lack of a response in six patients was attributed to their poor general state. The present results based on a prospective study demonstrate that PVP can be carried out safely and shows marked efficacy, in particular fast-acting pain relief, provided that patient and equipment selection is appropriate and that an experienced physician is available. Since PVP is a therapeutic technique, its safety cannot be evaluated like that of a phase I trial for drugs in which drug doses are increased incrementally to determine the optimal doses to be administered. Therefore, in the present study, we adopted a modified design of phase I study for drugs. However, the number of cases in our study is not enough to confirm the safety of PVP. Additionally, the results of this study are insufficient to establish PVP as a standard therapy for patients with painful malignant vertebral body tumors. Thus, we are planning to conduct a phase III study comparing PVP and conventional treatments in this context.

conclusion

PVP was proved safe, clinically efficacious, and fast acting in this prospective study. Future studies enrolling larger groups of patients will be needed to further establish its role in the management of painful bone lesions as palliative care.

acknowledgements

This study is the first prospective one to evaluate the safety and efficacy of PVP as palliative care for end-stage cancer patients. The authors have received no funds related to this study and are aware of no conflict of interest. A part of this study was shown as a poster presentation at the meeting of the American Society of Clinical Oncology, Chicago 2007.

references

1. Bates T. A review of local radiotherapy in the treatment of bone metastases and cord compression. Int J Radiat Oncol Biol Phys 1992; 23: 217–221.
2. Ben-Josef E, Shamsa F, Williams O et al. Radiotherapeutic management of osseous metastases: a survey of current patterns of care. Int J Radiat Oncol Biol Phys 1998; 40: 915–921.
3. Deramond H, Depriester C, Galibert P et al. Percutaneous vertebroplasty with polymethylmethacrylate. technique, indication, and results. Radiol Clin North Am 1998; 36: 533–546.
4. Cotton A, Boutry N, Cortet B et al. Percutaneous vertebroplasty: state of the art. Radiographics 1998; 18: 311–320.
5. Barr JD, Barr MS, Lemley TJ et al. Percutaneous vertebroplasty for pain relief and spinal stabilization. Spine 2000; 25: 923–928.
6. Weill A, Chiras J, Simon JM et al. Spinal metastases; indications for and results of percutaneous injection of acrylic surgical cement. Radiology 1996; 199: 241–247.
7. Murphy KJ, Deramond H. Percutaneous vertebroplasty in benign and malignant disease. Neuroimaging Clin N Am 2000; 10: 535–545.
8. Baba K, Ookubo K, Hamada K et al. Percutaneous vertebroplasty for osteolytic metastasis: a case report. Radiat Med 1997; 57: 880–882.
9. Kobayashi T, Takanaka T, Matsui O et al. Efficacy of percutaneous vertebroplasty under CT fluoroscopic guidance. Jpn J Intervent Radiol 1999; 14: 343–348.
10. Kobayashi T, Takanaka T, Matsui O et al. Practice of percutaneous vertebroplasty. Jpn J Intervent Radiol 2002; 17: 17–22.
11. Jensen ME, Kallmes DE. Percutaneous vertebroplasty in the treatment of malignant spine disease. Cancer J 2002; 8: 194–206.
12. Scroop R, Eskridge J, Britz GW. Paradoxical cerebral arterial embolization of cement during intraoperative vertebroplasty: case report. AJNR Am J Neuroradiol 2002; 23: 868–870.
13. Kaaufmann TJ, Jensen ME, Ford G et al. Cardiovascular effects of polymethyl methacrylate use in percutaneous vertebroplasty. AJNR Am J Neuroradiol 2002; 23: 601–604.
14. Wewers ME, Lowe NK. A critical review of visual analogue scales in the measurement of clinical phenomena. Res Nurs Health 1990; 13: 227–236.
15. http://ctep.cancer.gov/protocolDevelopment/electronic_applications/docs/ctcv20_4-30-992.pdf (15 April 2009, date last accessed).

Cardiovasc Intervent Radiol
DOI 10.1007/s00270-010-9817-y

CASE REPORT

Posterior Reversible Encephalopathy Syndrome Occurring After Uterine Artery Embolization for Uterine Myoma

Satoshi Suzuki · Noboru Tanigawa · Syuji Kariya · Atsushi Komemushi · Hiroyuki Kojima · Takanori Tokuda · Masanobu Kishimoto · Atsutoshi Tomino · Masayuki Fujioka · Yasuhide Kitazawa · Satoshi Sawada

Received: 26 August 2009 / Accepted: 30 December 2009

Abstract This case report describes posterior reversible encephalopathy syndrome (PRES) occurring after uterine artery embolization (UAE) for uterine myoma. This is the first report of PRES occurring after uterine vascular radiologic intervention. The mechanism by which UAE induced PRES is unclear.

Keywords Urinary artery embolization · Posterior reversible encephalopathy · Complication

Introduction

Posterior reversible encephalopathy syndrome (PRES) is clinically characterized by headache, seizures, visual disturbances, and mental disorder, along with specific findings on magnetic resonance imaging (MRI). These findings typically show as transient signal hyperintensity in the occipital lobe on fluid-attenuated inversion recovery (FLAIR) imaging and varying degrees of signal intensity on diffusion-weighted imaging. PRES has various etiologies, including hypertension; eclampsia and pre-eclampsia; immunosuppressive medications, such as cyclosporine; various antineoplastic agents; thrombocytopenic syndromes; Henoch-Schonleion purpura; systemic lupus erythematosus (SLE); and various conditions of renal failure [1]. The acronym "PRES" indicates the potentially reversible nature of the appearance on imaging and the symptomatology. Recently, transient cortical blindness (TCB), which has been recognized as a complication of contrast material administration, has been regarded as being a part of PRES. Many investigators have reported cases of TCB occurring after cerebrovascular and cardiovascular angiography [2]. However, to the best of our knowledge, PRES occurring after UAE has not been reported previously.

S. Suzuki (✉) · N. Tanigawa · S. Kariya · A. Komemushi · H. Kojima · T. Tokuda · S. Sawada
Department of Radiology, Kansai Medical University, Osaka, Japan
e-mail: sansansan33@hotmail.com

S. Suzuki · M. Kishimoto · A. Tomino · Y. Kitazawa
Department of Emergency and Critical Care Medicine, Kansai Medical University, Osaka, Japan

M. Fujioka
Stroke Center, Helios General Hospital, Dresden University of Technology, Saxony, Germany

Case Report

A 35-year-old woman was admitted for UAE of a giant uterine myoma, which measured 14 × 10 cm. In addition, she was receiving anticoagulation therapy with warfarin for chronic pulmonary embolism. Protein C deficiency had been identified 1 year earlier. Her cardiac duplex sonography showed mild pulmonary hypertension, and her estimated systolic pulmonary artery pressure was 40 mm Hg. However, there was no patent foramen ovale. Because she was on anticoagulative therapy, the patient opted for UAE rather than surgery as a treatment for uterine myoma. Physical examination disclosed neither pathogenic findings nor high blood pressure. Laboratory data on admission were within normal limits, with the exception of a prolonged prothombin time. No evidence of vasculitis or coagulation abnormality, including protein C activity, was identified. The procedure was performed using a right common femoral artery approach.

A 5F pigtail catheter (Cook, Bloomington, IN) was positioned at the level of the renal arteries to perform an

Published online: 12 February 2010

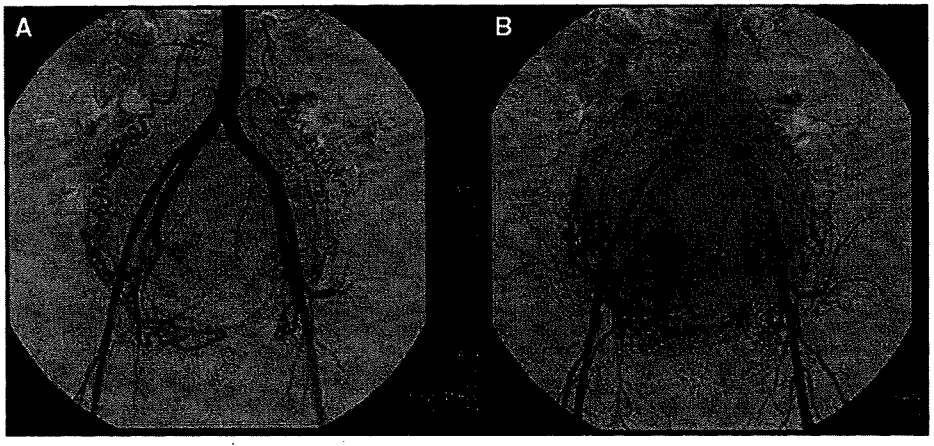

Fig. 1 Digital subtraction aortogram before embolization. **A** Arterial phase. **B** Early venous phase. No arterial venous fistula was present

abdominal aortogram. Both ovarian arteries were visualized during aortic injection and showed no arterial venous fistula (Fig. 1). Two 5F cobra-shaped angiographic catheters (C2 catheter; Clinical Supply, Gifu, Japan) catheterized to bilateral internal iliac arteries respectively. A Progreat microcatheter (Terumo, Tokyo, Japan) was advanced coaxially through the C2 catheter into the proximal uterine artery. Embolization was performed using porous gelatin microparticles (Jellpart; Astellas, Tokyo, Japan). The uterine myoma was successfully embolized. The total dose of ioversol contrast material (Optiray; Tyco Healthcare Japan, Tokyo, Japan) used was 186 ml. During the procedure, the patient's blood pressure increased to 166/83 mm Hg. After the procedure, she complained of severe headache with nausea and fell into a state of confusion. Two hours later, she developed convulsive seizures that were resistant to benzodiazepine and phenytoin. We therefore administered 1.2 g/d thyamiral (Citozol; Kyorin, Tokyo, Japan) to maintain sedation and also provided artificial ventilation support.

After the procedure, her systolic pressure did not exceed 160 mm Hg. Barbiturate therapy resolved the seizures. Cerebrospinal fluid was examined but showed no abnormalities. The first computed tomography (CT) scan showed contrast material remaining in the vessels, which were both arteries and venous sinus, without findings of hemorrhage (Fig. 2). MRI showed an area of increased T2-weighted and FLAIR signal intensity in the left occipital lobe (Fig. 3). Diffusion-weighted imaging (DWI) showed subtle signal hyperintensity in the corresponding area. Signal hyperintensity on DWI had faded by intensive care unit (ICU) day 7. On that day, barbiturate therapy was discontinued, and the ventilator was removed. Although the patient experienced no further epileptic episodes, she complained of distorted vision in the left eye and reported visual hallucinations of unrelated meaningful character string text on the wall and ceiling. Psychological and ophthalmological investigations showed no abnormalities. Symptoms gradually ameliorated and ceased by ICU day 10. Subsequent MRI on ICU day 14 showed that all abnormal findings on FLAIR and DWI had completely disappeared. She was discharged without sequelae.

Fig. 2 The first CT showed contrast material remaining in the vessels, which were both arteries and venous sinus, without findings of hemorrhage

Discussion

Typical symptoms of PRES are visual changes or transient blindness, seizures, headache, and unconsciousness [1]. The major cause of PRES is hypertension, which can be related to renal insufficiency, pre-eclampsia, or eclampsia.

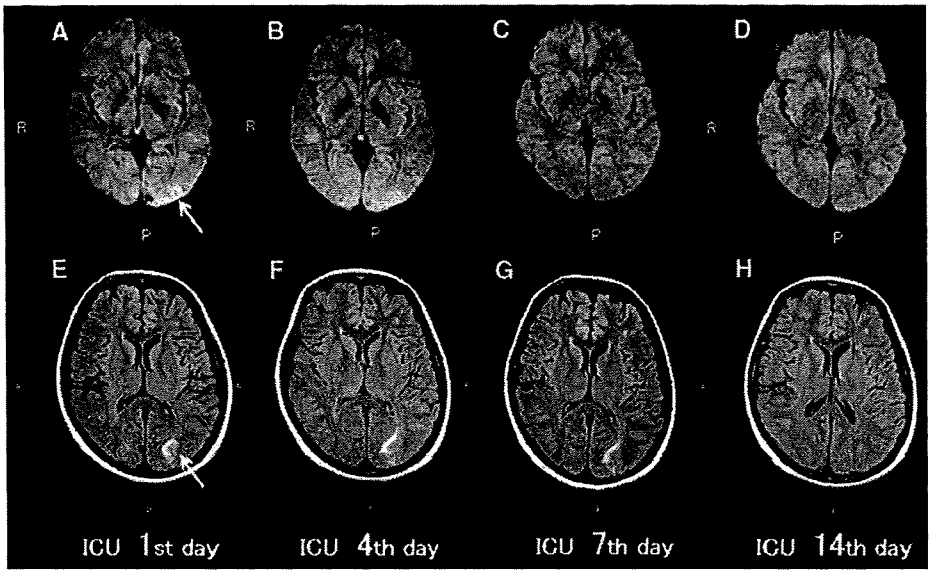

Fig. 3 **A** DWI on ICU day 1 showed a subtle high-signal intensity area in the left occipital lobe (*arrow*). **B** The subtle high-signal intensity area was still present on ICU day 4. **C** The high-signal intensity on DWI faded by ICU day 7. **D** DWI on ICU day 14. **E** FLAIR on ICU day 1 showed high-signal intensity in the left occipital lobe (*arrow*). **F** The high-signal intensity on FLAIR faded on ICU day 4. **G** FLAIR on ICU day 7. **H** The high-signal intensity on FLAIR faded by ICU day 14

Increased cerebral blood flow disturbs the autoregulation of cerebral blood pressure maintained by endothelial cells and the blood–brain barrier. Failure of autoregulation and the blood–brain barrier may then induce cerebral edema and microhemorrhage [3].

Some immunosuppressive agents can damage the blood–brain barrier by various direct toxic effects on the vascular endothelium [4]. PRES is related to various systemic vascular diseases, such as microthrombosis, as in hemolytic uremic syndrome, Henoch-Schonleion purpura, and SLE [1]. Endothelial activation and injury likely result in vasculopathy with altered intrinsic vascular tone from expression of inflammatory cytokines (e.g., tumor-necrotizing factor, interleukin), endothelin-1, thromboxane-A2, nitric oxide, and prostacyclin. These factors, alone or in combination, would result in PRES [5].

Conversely, TCB is a well-recognized phenomenon after cerebrovascular and cardiovascular angiography [6]. Horwitz reported that the morbidity rate for TCB could be as high as 0.3% to 1% [7]. TCB is characterized by partial or complete loss of perceived vision, normal fundi, normal papillary reflexes, and unaltered extraocular movements. Intra-arterial contrast material apparently penetrates the blood–brain barrier by opening tight capillary junctions or enhancing endothelial pinocytosis [8]. In the present case, the fact that the first CT demonstrated contrast material in the cerebral vessels indicated that TCB would have been induced by injection of contrast material into the uterine artery. However, no previous reports have described TCB in association with seizures and loss of consciousness. We therefore diagnosed PRES in this case. In contrast, TCB resembles PRES symptomatologically and neuroradiologically and may share a common pathophysiology [2].

The mechanisms of PRES can be explained by two main hypotheses involving vascular permeability [9] and varying grades of ischemia [10]. Neuroradiologically, in PRES, MRI shows increased signal intensity on T2-weighted imaging and FLAIR in the corresponding area [10, 11]. These MRI findings are also distributed among the cerebellum, thalamus, brain stem, and basal ganglia. DWI shows relative smaller increases in signal intensity [12].

The present case is compatible with PRES. Signal hyperintensity on T2-weighted imaging and FLAIR was identified only in the occipital lobe, corresponding to clinical symptoms, and signal hyperintensity on DWI may be reflected by signal hyperintensity on T2-weighted imaging, i.e., "T2 shine-through phenomena." The distribution of hyperintensity of DWI does not correspond to posterior cerebral arterial territory. In addition, previous duplex sonography did not indicate the possibility of paradoxical embolization. Thus, we ruled out an ischemic event.

UAE has been introduced as an alternative to surgery for women with symptomatic uterine myoma and has rapidly gained in popularity. However, no previous reports have described TCB or PRES as complications of UAE [13, 14]. In this case, some relation may have existed between the procedure and PRES, but the pathology remains unclear. We suspect that some vasocontrictive factors related to the embolization procedure caused a vasoactive effect. Tissue levels of prostaglandin (PGF2a) are apparently increased in the uterus with myoma [15]. Serum PGF2a is known to affect systemic vasoconstriction and vasogenic edema as an inflammation mediator. PGF2a secreted from ischemic tissue in the uterine myoma may thus facilitate vasogenic changes in PRES.